ELSEVIER

Journal of Alloys and Compounds 390 (2005) 197–201

Journal of ALLOYS AND COMPOUNDS

www.elsevier.com/locate/jallcom

Intense visible fluorescence and energy transfer in Dy^{3+}, Tb^{3+}, Sm^{3+} and Eu^{3+} doped rare-earth borate glasses

Hai Lin[a,b,*], Edwin Yue-Bun Pun[b], Xiaojun Wang[c], Xingren Liu[c]

[a] *Faculty of Chemical Engineering and Materials, Dalian Institute of Light Industry, Dalian 116034, PR China*
[b] *Department of Electronic Engineering, City University of Hong Kong, Tat Chee Avenue, Kowloon, Hong Kong, PR China*
[c] *Changchun Institute of Optics, Fine Mechanics and Physics, Chinese Academy of Sciences, Changchun 130021, PR China*

Received 16 April 2004; accepted 6 July 2004

Abstract

Tb^{3+}/Dy^{3+} and Eu^{3+}/Sm^{3+} doped rare-earth borate glasses have been synthesized and characterized. Under UV excitation, Dy^{3+}, Tb^{3+}, Sm^{3+} and Eu^{3+} emit intense yellowish white, green, reddish orange and red lights, respectively. In Tb^{3+}/Dy^{3+} co-doped glasses, the enhancement of Tb^{3+} green emission is observed, and the sensitization is related to the efficient energy transfer from Dy^{3+} to Tb^{3+}. In Eu^{3+}/Sm^{3+} co-doped glasses, the excitation wavelength range of Eu^{3+} emission is broadened owing to the energy transfer from Sm^{3+} to Eu^{3+}. This broadening makes the Ar^{+} 488 nm wavelength laser a powerful excitation source for Eu^{3+} fluorescence. The rare-earth doped glasses with various visible emissions are useful for developing new color light sources, fluorescent display devices, UV-sensor and tunable visible lasers.

Keywords: A. Amorphous materials; B. Chemical synthesis; D. Luminescence

1. Introduction

Rare-earth doped glasses are useful materials for bulk lasers, optical fibers, waveguide lasers and optical amplifiers [1–3]. Trivalent rare-earth ions Er and Tm doped phosphate, silicate, gemanite and tellurite glasses have been developed for infrared active optical devices [4–8]. Recently, research focus on rare-earth doped glasses is not limited to infrared optical devices, and there is a growing interest in visible optical devices [9–10]. With the increasing demand of various visible lasers and light sources, further investigations in other rare-earth ions, such as Dy, Tb, Sm and Eu ions, are becoming more important [11–17].

Good glass host is very important for efficient luminescence of rare-earth ions. Borate glass is a suitable optical material with high transparency, low melting point, high thermal stability and good rare-earth ions solubility [17,18]. However, interest in borate glass is small due to its high phonon energy, and it is difficult to obtain high efficient infrared and upconversion visible emissions in Er, Tm and Ho ions. On the other hand, the high phonon energy in borate glass is not detrimental to Dy, Tb, Sm and Eu normal 4f transitions, and sometimes it can accelerate the relaxation process, which is necessary and beneficial for visible emissions. In this work, borate glass as a suitable host for Dy, Tb, Sm and Eu rare-earth ions is demonstrated. Efficient yellowish white, green, reddish orange and red lights were measured and characterized. In Tb/Dy co-doped glass system, enhancement of Tb^{3+} green emission is observed, and the sensitization is due to the efficient energy transfer from Dy^{3+} to Tb^{3+}. In Eu/Sm co-doped glass system, the excitation wavelength range of Eu^{3+} emission is broadened owing to the energy transfer from Sm^{3+} to Eu^{3+}. These rare-earth doped borate glasses with various visible emissions will be useful in developing new light sources, display devices, UV-sensors and tunable visible lasers.

2. Experiments

The molar compositions of Dy^{3+} and Tb^{3+} doped Li_2O–BaO–La_2O_3–B_2O_3 (LBLB) glasses are

* Corresponding author. Tel.: +86 411 86323649; fax: +86 411 86323038.
E-mail address: lhai@dlili.edu.cn (H. Lin).

0925-8388/$ – see front matter © 2004 Elsevier B.V. All rights reserved.
doi:10.1016/j.jallcom.2004.07.068

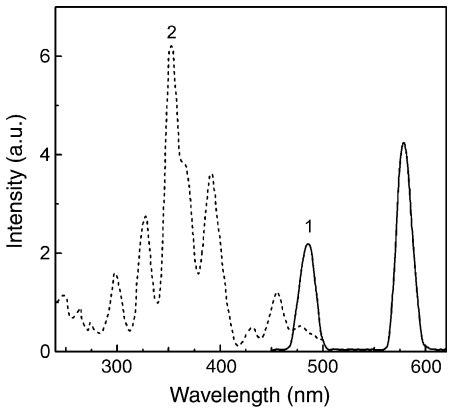

Fig. 1. Emission spectrum under 358 nm UV excitation (curve 1) and excitation spectrum for 580 nm emission in Dy^{3+} doped LBLB glasses (curve 2).

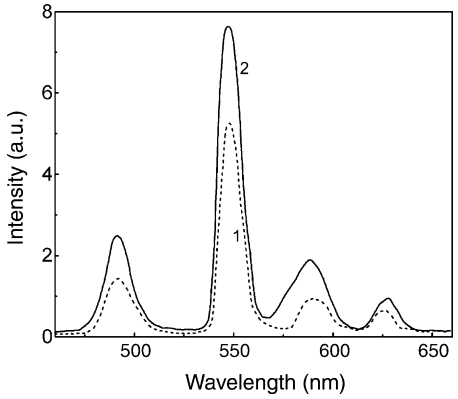

Fig. 2. Emission spectra of Tb^{3+} doped (curve 1) and Tb^{3+}/Dy^{3+} co-doped (curve 2) LBLB glasses under 358 nm UV excitation.

$8Li_2O{\cdot}7BaO{\cdot}(15-x-y)La_2O_3{\cdot}70B_2O_3{:}xDy^{3+},\ yTb^{3+}$. For the samples reported here, $x=0.1$ and $y=0$, $x=0$ and $y=1$, and $x=0.1$ and $y=1$, respectively. The molar compositions of Sm^{3+} and Eu^{3+} doped LBLB glasses are $8Li_2O{\cdot}7BaO{\cdot}(15-m-n)La_2O_3{\cdot}70B_2O_3{:}mSm^{3+},\ nEu^{3+}$, and here, $m=0.1$ and $n=0$, $m=0$ and $n=1$, and $m=0.1$ and $n=1$, respectively. All the chemical powders were of 99.5–99.999% purity. The well-mixed raw materials were first heated for 30 min in an Al_2O_3 crucible at 800 °C using an electric furnace, and then at a higher melting temperature of 1150 °C for 2 h. LBLB:Tb^{3+} and LBLB:Dy^{3+}, Tb^{3+} glasses were prepared in a reducing atmosphere (CO gas) because Tb_4O_7 was used as raw material for Tb^{3+} ions. The glasses were obtained by pouring the melt into a preheated brass mould. The samples were subsequently annealed at lower temperatures and then sliced and polished. The excitation and fluorescence spectra of the samples were measured at room temperature using a Hitachi MPF-4 spectrophotometer and a 75-W xenon lamp source.

3. Results and discussion

3.1. Dy^{3+} and Tb^{3+} doped LBLB glasses

Dy^{3+} and Tb^{3+} single doped LBLB glasses emit bright yellowish white and green lights, respectively. Curve 1 in Fig. 1 shows the emission spectrum of LBLB:Dy^{3+} glass under 358 nm excitation. The yellowish white light is composed of 486 nm (blue) and 579 nm (yellow) emission bands. The two bands correspond to the $^4F_{9/2} \rightarrow {}^6H_{15/2}$ and $^4F_{9/2} \rightarrow {}^6H_{13/2}$ optical transitions, respectively, and the full width at half maximum (FWHM) is 18 nm in both cases. The integrated intensity ratio between the yellow and blue bands is 1.9:1. The excitation spectrum of the yellow emission is shown in curve 2. In the spectral region from 280 to 500 nm, there are eight excitation bands situating at 299, 328, 352, 364, 391, 431, 455 and 479 nm. The 431, 455 and 479 nm bands are associated with the transitions from the ground level $^6H_{15/2}$ to $^4G_{11/2}$, $^4I_{15/2}$ and $^4F_{9/2}$ levels, respectively, and other bands are associated with the transitions from the ground level to other higher 4f excited levels, respectively. Efficient excitation of Dy^{3+} with UV radiation is confirmed here.

The emission spectrum of LBLB:Tb^{3+} under 358 nm UV excitation is shown as curve 1 in Fig. 2. It consists of four emission bands, locating at 492, 547, 590 and 626 nm and belonging to the $^5D_4 \rightarrow {}^7F_J$ ($J=6, 5, 4, 3$) transitions, respectively. The most intense emission peak is at 547 nm, and its FWHM is only 13 nm. The peak intensity is >2 times higher than other peaks, hence the fluorescence color is near pure green. The emission spectrum of Dy^{3+} and Tb^{3+} co-doped LBLB glasses under 358 nm UV radiation is given as curve 2. Spectral comparison in Fig. 2 shows that co-doping with a small amount of Dy^{3+} ions enhances the Tb^{3+} green emission bands. In the co-doped sample, the 547 nm emission peak is 45% higher than that in the single doped one. This enhancement is due to the small amount of co-dopant Dy^{3+}, and is not due to the Dy^{3+} fluorescence overlap because there is no 547 nm emission for Dy^{3+} ion.

Fig. 3 gives the excitation spectra of Tb^{3+} green emission in Tb^{3+} single doped (curve 1) and Dy^{3+} and Tb^{3+}

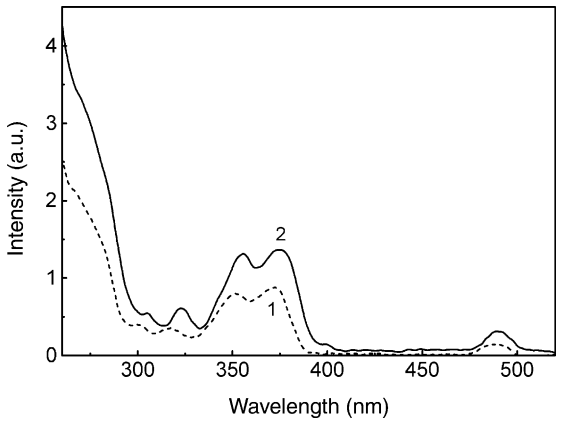

Fig. 3. Excitation spectra for 547 nm emission in Tb^{3+} doped (curve 1) and Tb^{3+}/Dy^{3+} co-doped (curve 2) LBLB glasses.

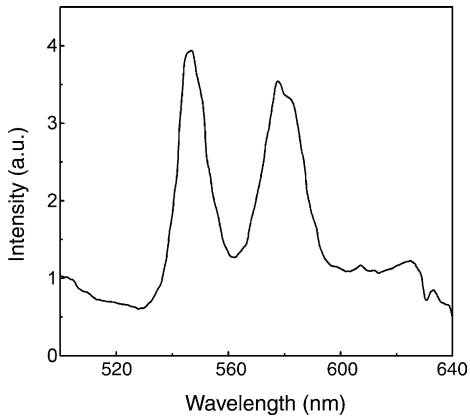

Fig. 4. Emission spectra of Tb^{3+}/Dy^{3+} co-doped LBLB glasses under 453 nm blue light excitation.

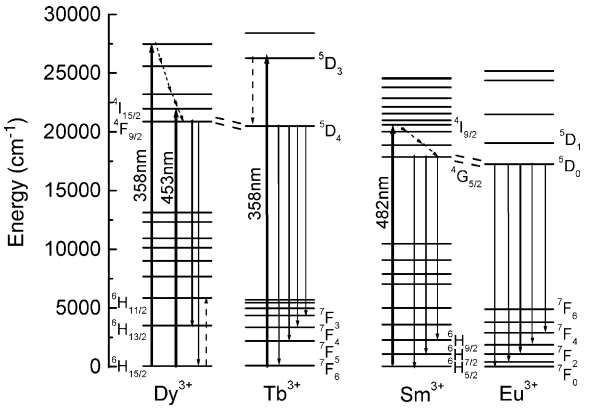

Fig. 5. Energy level diagrams and visible emission transitions for Dy^{3+}, Tb^{3+}, Sm^{3+} and Eu^{3+}. Energy transfer processes from Dy^{3+} to Tb^{3+} and from Sm^{3+} to Eu^{3+} are indicated.

co-doped (curve 2) LBLB glasses. In the 300–500 nm spectral region, there are five excitation bands at 300, 318, 352, 373 and 490 nm in Tb^{3+} single doped system. The 352, 373 and 490 nm bands are associated with the transitions from the ground level $^7F_6$ to $^5D_2$, $^5D_3$ and $^5D_4$ levels, respectively, and other bands are owing to the transitions from the ground level to other higher 4f excited levels, respectively. The 547 nm emission intensity in co-doped glass is much higher than that in single doped glass under the UV light excitation. The comparison of both emission and excitation spectra indicates that Dy^{3+} ions sensitize the fluorescence of Tb^{3+} efficiently.

The energy transfer from Dy^{3+} to Tb^{3+} is the reason for efficient luminescence sensitization. To confirm this, 453 nm blue light was selected as an excitation source. Excitation spectrum of Tb^{3+} shows that LBLB:Tb^{3+} glass does not emit light under this excitation condition. For LBLB:Dy^{3+}, Tb^{3+} glass, there is 578 nm yellow emission from Dy^{3+} and 547 nm green and weaker 626 nm red emissions from Tb^{3+}, as shown in Fig. 4. The appearance of Tb^{3+} emission bands indicates that a part of the absorption energy of Dy^{3+} has been transferred to Tb^{3+}.

Energy transfer process from Dy^{3+} to Tb^{3+} is described in the energy level diagram, as shown in Fig. 5 [11,19,20]. When the 4f higher energy level of Dy^{3+} is excited with 358 nm wavelength light, the initial population relaxes to lower energy levels until it arrives at the $^4F_{9/2}$ level by phonon assistance. With the emission of phonons, part of the energy in the $^4F_{9/2}$ level of Dy^{3+} is transferred to the $^5D_4$ level of Tb^{3+} by resonance between the two energy levels. The energy transfer from Dy^{3+} to Tb^{3+} is almost irreversible, because the $^4F_{9/2}$ level in Dy^{3+} is about 400 cm^{-1} higher than the $^5D_4$ level in Tb^{3+}, and the probability in emitting phonons for Dy^{3+} $^4F_{9/2} \rightarrow Tb^{3+}$ $^5D_4$ process is much higher than that in capturing phonons for Tb^{3+} $^5D_4 \rightarrow Dy^{3+}$ $^4F_{9/2}$ process. The energy resonance transfer enhances the population of Tb^{3+} $^5D_4$ levels. In addition, the energy gap between the $^5D_3$ and $^5D_4$ levels in Tb^{3+} matches with the gap between the $^6H_{11/2}$ and $^6H_{15/2}$ levels in Dy^{3+}. Thus, cross-relaxation between Dy^{3+} and Tb^{3+} exists and the population of Tb^{3+} $^5D_4$ levels is increased. The total increment of the population due to the co-doping with Dy^{3+} leads to the sensitization of fluorescence in Tb^{3+}.

3.2. Sm^{3+} and Eu^{3+} doped LBLB glasses

Sm^{3+} and Eu^{3+} single doped LBLB glasses emit reddish orange and red lights, respectively. The emission spectra of Sm^{3+} and Eu^{3+} in LBLB glasses under blue and UV light excitation are shown in Fig. 6. The reddish orange light of Sm^{3+} (curve 1) is composed of 563, 600 and 646 nm emission bands, corresponding to the $^4G_{5/2} \rightarrow {}^6H_J$ ($J = 5/2$, 7/2 and 9/2) transitions, respectively. The 600 nm emission band is the most intense and its FWHM is 17 nm. Curve 2 shows the emission spectrum of Eu^{3+} in LBLB glasses under 397 nm excitation. It is composed of 577, 591, 615, 654 and 702 nm emission bands. They belong to the $^5D_0 \rightarrow {}^7F_J$ ($J = 0$, 1, 2, 3, 4) transitions, respectively, and the main emission is the 615 nm red band.

The excitation spectra of 650 nm emission in Sm^{3+} and 597 nm emission in Eu^{3+} in LBLB glasses are given in Fig. 7. The excitation spectrum of Sm^{3+} (curve 1) is composed of

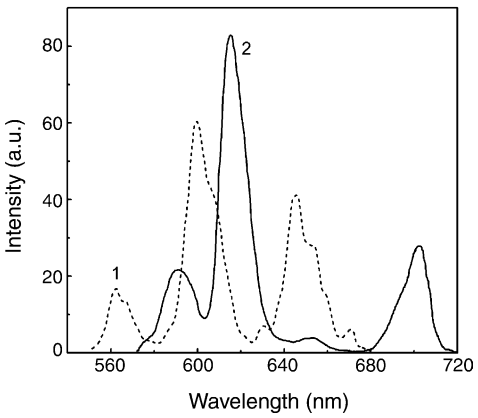

Fig. 6. Emission spectra of Sm^{3+} under 410 nm excitation (curve 1) and of Eu^{3+} under 397 nm excitation (curve 2).

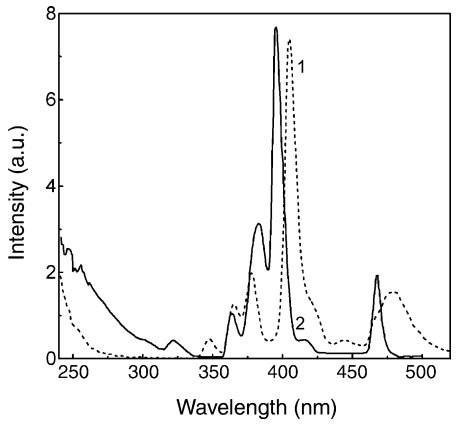

Fig. 7. Excitation spectra for 650 nm emission in Sm^{3+} (curve 1) and 597 nm emission in Eu^{3+} (curve 2) in single doped LBLB glasses.

eight bands peaking at ~240, 348, 365, 378, 405, 421, 445 and 479 nm, respectively. The broadband at ~240 nm is due to charge transfer state (CTS) of Sm^{3+}, and other sharp peaks are due to the 4f–4f inner shell transitions of Sm^{3+}. The excitation spectrum of Eu^{3+} (curve 2) consists of eight bands peaking at ~240, 321, 364, 383, 395, 416, 421 and 468 nm, respectively. The broadband at ~240 nm and other seven peaks are due to the CTS and the 4f–4f transitions of Eu^{3+}.

Similar to Tb^{3+}/Dy^{3+} co-doped system, energy transfer has also been observed in Eu^{3+}/Sm^{3+} co-doped LBLB glasses. The energy transfer occurs when 482 nm blue light was used as an excitation source. Under this excitation condition, there is no emission in Eu^{3+} single doped LBLB glass because 482 nm wavelength is outside the Eu^{3+} excitation range as shown above. However, in Eu^{3+}/Sm^{3+} co-doped system, 565, 600 and 646 nm emissions from Sm^{3+} plus 615 and 702 nm emissions from Eu^{3+} are observed, as shown in Fig. 8. The Eu^{3+} emission bands appearing in the Sm^{3+} emission spectrum indicates that a part of the absorption energy of Sm^{3+} has been transferred to Eu^{3+}. In particular, the most intensive emission in the spectrum is the 615 nm red peak of Eu^{3+}, and it confirms that the energy transfer from

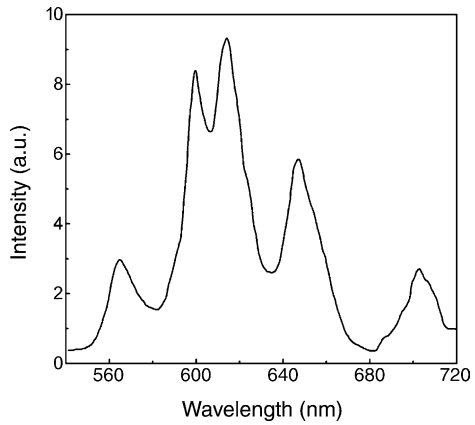

Fig. 8. Emission spectrum of Eu^{3+}/Sm^{3+} co-doped LBLB glasses under 482 nm excitation.

Sm^{3+} to Eu^{3+} is efficient. The existence of energy transfer expands the selectable pump source wavelength range for Eu^{3+} fluorescence. Hence, the 488 nm wavelength from argon laser is a powerful excitation source for Eu^{3+} red emission in Eu^{3+}/Sm^{3+} co-doped LBLB glass systems.

The energy transfer process from Sm^{3+} to Eu^{3+} is also shown in Fig. 5. When the $^4I_{9/2}$ level of Sm^{3+} is excited with 482 nm blue light, the initial population relaxes finally to the $^4G_{5/2}$ level. Part of the energy in the $^4G_{5/2}$ level of Sm^{3+} is transferred to the $^5D_0$ level of Eu^{3+} by resonance between the two energy levels. The energy transfer from Sm^{3+} to Eu^{3+} is almost irreversible, because the $^4G_{5/2}$ level in Sm^{3+} is about 600 cm^{-1} higher than the $^5D_0$ level in Eu^{3+}, and the probability in emitting phonons for Sm^{3+} $^4G_{5/2} \rightarrow Eu^{3+}$ $^5D_0$ process is much higher than that in capturing phonons for Eu^{3+} $^5D_0 \rightarrow Sm^{3+}$ $^4G_{5/2}$ process. The energy resonance transfer enhances the population of Eu^{3+} $^5D_0$ level. The increment of the population due to the co-doping with Sm^{3+} causes the sensitization of Eu^{3+} emission under certain excitation conditions, and leads to the expansion of excitation range in Eu^{3+} fluorescence.

4. Conclusions

Dy^{3+}, Tb^{3+}, Sm^{3+} and Eu^{3+} doped borate glasses have been synthesized and characterized. In single doped glasses, Dy^{3+}, Tb^{3+}, Sm^{3+} and Eu^{3+} emit intense yellowish white, green, reddish orange and red lights under UV and blue light excitation, respectively. Enhancement of Tb^{3+} green emission is observed in Tb^{3+}/Dy^{3+} co-doped glass systems, and the sensitization is due to the efficient energy transfer from Dy^{3+} to Tb^{3+}. For Eu^{3+}/Sm^{3+} system, the excitation wavelength range for Eu^{3+} emission is broadened due to the energy transfer from Sm^{3+} to Eu^{3+}. The broadening makes the 488 nm wavelength Ar^+ laser a powerful source for Eu^{3+} fluorescence. These glasses can be excited efficiently using commercial UV and blue laser diodes and LEDs, and can be used for developing new color light sources, fluorescent display devices, UV-sensors and tunable visible lasers.

References

[1] P.R. Biju, G. Jose, V. Thomas, V.P.N. Nampoori, N.V. Unnikrishnan, Opt. Mat. (2004) 24.
[2] S.D. Jackson, Appl. Phys. Lett. 83 (2003) 1316–1318.
[3] B.N. Samson, J.A. Medeiros Neto, R.I. Laming, D.W. Hewak, Electron. Lett. 30 (1994) 1617–1618.
[4] A. Mori, K. Kobayashi, M. Yamada, T. Kanamori, K. Oikawa, Y. Nishida, Y. Ohishi, Electron. Lett. 34 (1998) 887–888.
[5] H. Lin, E.Y.B. Pun, S.Q. Man, X.R. Liu, J. Opt. Soc. Am. B 18 (2001) 602–609.
[6] G. Jose, G. Sorbello, S. Taccheo, E. Cianci, V. Foglietti, P. Laporta, J. Non Cryst. Solids 322 (2003) 256–261.
[7] N.O. Dantas, F. Qu, J.T. Arantes Jr., J. Alloy Compd. 344 (2002) 316–319.

[8] S. Tanabe, X. Feng, T. Hanada, Opt. Lett. 25 (2000) 817–819.
[9] J. Hao, J. Gao, M. Cocivera, Appl. Phys. Lett. 82 (2003) 2224–2226.
[10] S. Schweizer, L.W. Hobbs, M. Secu, J. Spaeth, A. Edgar, G.V.M. Williams, Appl. Phys. Lett. 83 (2003) 449–451.
[11] J.B. Gruber, B. Zandi, U.V. Valiev, Sh.A. Rakhimov, J. Appl. Phys. 94 (2003) 1030–1034.
[12] D.A. Turnbull, S.Q. Gu, S.G. Bishop, J. Appl. Phys. 80 (1996) 2436–2441.
[13] D. Ruter, W. Bauhofer, Appl. Phys. Lett. 69 (1996) 892–894.
[14] L. de S. Menezes, G.S. Maciel, Cid B. de Araujo, Y. Messaddeq, J. Appl. Phys. 94 (2003) 863–866.
[15] I.R. Martin, A.C. Yanes, J. Mendez-Ramos, M.E. Torres, V.D. Rodriguez, Appl. Phys. Lett. 89 (2001) 2520–2524.
[16] H. Lin, E.Y.B. Pun, L.H. Huang, X.R. Liu, Appl. Phys. Lett. 80 (2002) 2642–2644.
[17] N. Soga, K. Hirao, M. Yoshimoto, H. Yamamoto, J. Appl. Phys. 63 (1988) 4451–4454.
[18] S.M. Kaczmarek, Opt. Mat. 19 (2002) 189–194.
[19] W.T. Carnall, P.R. Fields, K. Rajnak, J. Chem. Phys. 49 (1968) 4412–4423.
[20] W.T. Carnall, P.R. Fields, K. Rajnak, J. Chem. Phys. 49 (1968) 4424–4442.